



AFRL-OSR-VA-TR-2014-0168

---

**Chemical Dynamics at Surfaces of Metal Nanomaterials**

**Junrong Zheng**  
**WILLIAM MARSH RICE UNIV HOUSTON TX**

---

**07/23/2014**  
**Final Report**

DISTRIBUTION A: Distribution approved for public release.

Air Force Research Laboratory  
AF Office Of Scientific Research (AFOSR)/ RTE  
Arlington, Virginia 22203  
Air Force Materiel Command

# REPORT DOCUMENTATION PAGE

Form Approved  
OMB No. 0704-0188

Public reporting burden for this collection of information is estimated to average 1 hour per response, including the time for reviewing instructions, searching existing data sources, gathering and maintaining the data needed, and completing and reviewing this collection of information. Send comments regarding this burden estimate or any other aspect of this collection of information, including suggestions for reducing this burden to Department of Defense, Washington Headquarters Services, Directorate for Information Operations and Reports (0704-0188), 1215 Jefferson Davis Highway, Suite 1204, Arlington, VA 22202-4302. Respondents should be aware that notwithstanding any other provision of law, no person shall be subject to any penalty for failing to comply with a collection of information if it does not display a currently valid OMB control number. **PLEASE DO NOT RETURN YOUR FORM TO THE ABOVE ADDRESS.**

<b>1. REPORT DATE (DD-MM-YYYY)</b>		<b>2. REPORT TYPE</b>	<b>3. DATES COVERED (From - To)</b>		
<b>4. TITLE AND SUBTITLE</b>			<b>5a. CONTRACT NUMBER</b>		
			<b>5b. GRANT NUMBER</b>		
			<b>5c. PROGRAM ELEMENT NUMBER</b>		
<b>6. AUTHOR(S)</b>			<b>5d. PROJECT NUMBER</b>		
			<b>5e. TASK NUMBER</b>		
			<b>5f. WORK UNIT NUMBER</b>		
<b>7. PERFORMING ORGANIZATION NAME(S) AND ADDRESS(ES)</b>			<b>8. PERFORMING ORGANIZATION REPORT NUMBER</b>		
<b>9. SPONSORING / MONITORING AGENCY NAME(S) AND ADDRESS(ES)</b>			<b>10. SPONSOR/MONITOR'S ACRONYM(S)</b>		
			<b>11. SPONSOR/MONITOR'S REPORT NUMBER(S)</b>		
<b>12. DISTRIBUTION / AVAILABILITY STATEMENT</b>					
<b>13. SUPPLEMENTARY NOTES</b>					
<b>14. ABSTRACT</b>					
<b>15. SUBJECT TERMS</b>					
<b>16. SECURITY CLASSIFICATION OF:</b>			<b>17. LIMITATION OF ABSTRACT</b>	<b>18. NUMBER OF PAGES</b>	<b>19a. NAME OF RESPONSIBLE PERSON</b>
<b>a. REPORT</b>	<b>b. ABSTRACT</b>	<b>c. THIS PAGE</b>			<b>19b. TELEPHONE NUMBER (include area code)</b>

# Chemical Dynamics at Surfaces of Metal Nanomaterials

## – AFOSR 2011 YIP Award FA9550-11-1-0070 Final Report

Junrong Zheng  
Department of Chemistry, Rice University

### 1. Proposed summary

The project was designed to develop novel spectroscopic tools for the determinations of molecular structures and dynamics on the surfaces of metal nanomaterials – the critical component of heterogeneous catalysts, and to use the new tools to investigate whether a fundamental physical principle, the Born-Oppenheimer Approximation (BOA), is valid on the surfaces of these materials or not.

### 2. Achievements

During the past three years supported by the award (*FA9550-11-1-0070*), my group pioneered two novel molecular structural tools: (1) the vibrational cross angle method for the determination of 3D molecular structures<sup>1-5</sup>; and (2) the vibrational energy transfer method for the determination of intermolecular distances with an angstrom precision<sup>6-11</sup>. Using the methods, we showed that the 3D molecular conformations on metal nanomaterials with Au nanoparticles as examples can be directly determined<sup>3,5</sup>, and the validity of Born-Oppenheimer Approximation on the surfaces of metal nanomaterials is dependent on detailed molecular properties<sup>5,12-14</sup>, and the energy dissipation pathways in the systems largely depend on whether BOA is valid<sup>12-14</sup>. In the following, the accomplishments will be briefly described.

#### 2.1 The vibrational cross angle method to determine 3D molecular structures

One of the major problems in experimentally studying heterogeneous catalysis is the lack of tools for the determinations of molecular structures on the surfaces of metal nanomaterials. Practical catalysts, e.g. oxide-supported metal clusters, are polycrystalline solids. XRD cannot be used to resolve the molecular structures in such systems because they are not single crystals. NMR also has difficulties in determining molecular structures in them not only because the solid NMR has broad lineshapes, but also because the metal clusters typically have open shell electrons which can severely disrupt the magnetic fields on their surfaces. 1D vibrational methods, e.g. FTIR, Raman, or SFG, are usually used in monitoring the molecular changes in heterogeneous catalytic systems by obtaining the vibrational frequencies and peak intensities. However, the structural determination capability of the 1D vibrational techniques suffers from the fact that vibrational frequencies are severely affected by Fermi resonances because of which the vibrational frequency shifts can be more significant than those caused by molecular structural changes. Motivated by such a practical difficulty, my groups developed a vibrational cross angle method which is general for the determination of 3D molecular structures in condensed phases.

The principle of our method is by determining the cross angles between vibrational transition dipoles covering the entire molecular space to determine 3D molecular conformations (Fermi resonances don't affect the results from such a method),<sup>1-5</sup> with the aid of our unique powerful ultrafast multiple dimensional IR/THz spectroscopy setup<sup>3</sup> which solves a longstanding

problem: the lack of frequency tunable sources over the entire Mid-IR range with sufficient power has prevented essentially all other current 2D IR techniques from resolving 3D molecular structures because vibrational couplings with wide spatial or frequency separation cannot be observed or modes with weak transition dipole moments are too weak to be detected. The method has been benchmarked with well-defined crystalline samples,<sup>1,4</sup> and successfully applied to map the 3D molecular conformations in liquids,<sup>1</sup> solids<sup>1,4</sup> and on the surfaces of nanomaterials<sup>5</sup>.

Our recent work<sup>1</sup> will be used to demonstrate the method.

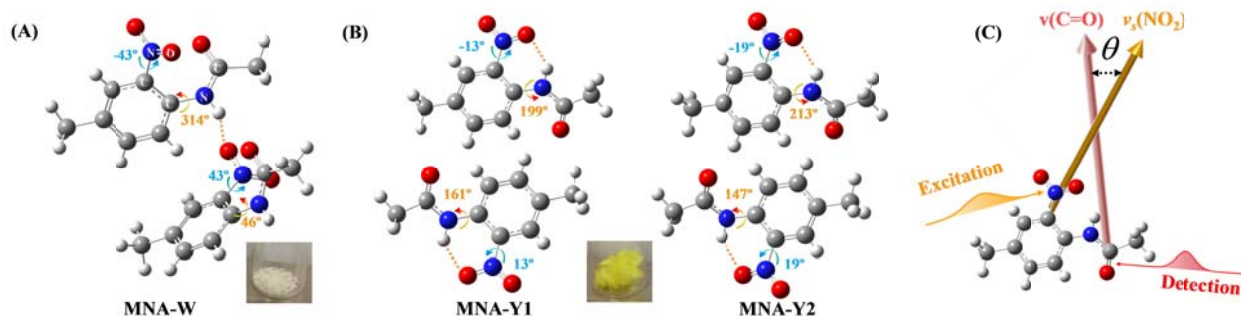


**Figure 1.** Molecular conformations of MNA in (A) the white crystal MNA-W, and (B) the yellow crystal. (C) Illustration of how the vibrational cross angle between two modes is experimentally determined.

Fig.1(A)&(B) display the molecular conformations of MNA (4'-Methyl-2'-nitroacetanilide) in two of its crystals (white and yellow as shown) determined by XRD. The conformations are defined by the two dihedral angles  $\angle CC/NO$  (between the benzene plane and the nitro plane) and  $\angle CC/NC$  (between the benzene plane and the amide plane). In the white crystal, there are one pair of chiral images, and in the yellow crystal there are two pairs. The molecule has many typical chemical bonds, e.g.  $C-C-H$ ,  $N=O$ ,  $C=C$ ,  $C=O$ ,  $N-H$  and  $C-O$ , which cover the three planes of the molecule. The relative orientations of the vibrations of these bonds can be utilized to obtain the molecular conformations in terms of the two dihedral angle values.

To determine the cross angle between two vibrations, as illustrated in fig.1(C), a linearly polarized IR pulse excites a vibrational mode (the  $NO_2$  stretch at  $1362\text{ cm}^{-1}$ ). After a very short period of time ( $0.1\sim 0.2\text{ps}$ ) before the molecular rotation or conformational changes have occurred for a substantial extent, another linearly polarized pulse of different frequencies detects a signal generated from the response of another vibrational mode (the  $C=O$  stretch) to the excitation of the  $NO_2$  stretch. In general, the excitation of one vibrational mode can lead to the vibrational frequency shift of another mode because of the anharmonic coupling. The coupling produces a cross peak pair in the experimental results as displayed in fig.2B. In fig.2B, the excitation frequency  $\omega_1 = 1362\text{ cm}^{-1}$  is the  $NO_2$  stretch 0-1 transition frequency, indicating that the cross peak pair is from the  $NO_2$  excitation. The detection frequency (red peak)  $\omega_3 = 1672\text{ cm}^{-1}$  is the  $C=O$  stretch 0-1 transition frequency, indicating that the cross peak pair is from the 0-1 transition frequency shift of the  $C=O$  stretch from  $1672\text{ cm}^{-1}$  (red peak) to  $1555\text{ cm}^{-1}$  (blue peak) caused by the  $NO_2$  excitation. The amplitudes of the cross peaks (fig.2D) are dependent on the polarizations of the exciting and detecting beams, and the cross angle  $\theta$  ( $0^\circ \leq \theta \leq 90^\circ$ ) between the transition dipole moment directions of the two coupled modes. For a

sample isotropically distributed within the laser focus spot, the vibration cross angle can be straightforwardly determined based on the relation:

$$\frac{I_{\perp}}{I_{\parallel}} = \frac{2 - \cos^2 \theta}{1 + 2 \cos^2 \theta} \quad \text{eq.1}$$

where  $I_{\parallel}, I_{\perp}$  are off-diagonal peak intensities with parallel and perpendicular excitation/detection polarizations, respectively. From both parallel and perpendicular measurements (fig.2D) and eq.1, the vibrational cross angle between the  $\text{NO}_2$  stretch and the  $\text{C}=\text{O}$  stretch is determined to be  $70^\circ \pm 2^\circ$ .

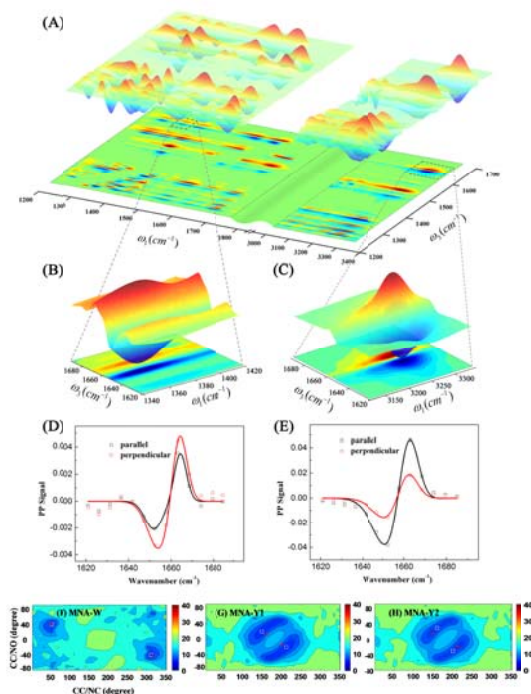


**Figure 2.** (A) Multiple-mode 2D IR spectrum of a polycrystalline sample of the MNA white crystal. (B) Enlarged 2D-IR spectrum for the cross peak pair  $\text{NO}_2/\text{C}=\text{O}$ , and (C) enlarged 2D-IR spectrum for the cross peak pair  $\text{NH}/\text{C}=\text{O}$ . (D) A slice cut along  $\omega_1 = 1362 \text{ cm}^{-1}$  of fig.2B with the polarization of the excitation both parallel ( $\parallel$ ) and perpendicular ( $\perp$ ) to the polarization of the detection beam and (E) A slice cut along  $\omega_1 = 3260 \text{ cm}^{-1}$  of fig.2C with both parallel and perpendicular configurations. The average difference between the experimental and calculated vibrational cross angles of MNA conformations with different  $\angle\text{CC}/\text{NO}$  and  $\angle\text{CC}/\text{NC}$  dihedral angles for (F) MNA-W, (G) MNA-Y1, and (H) MNA-Y2. The z-axis is the amplitude of difference. The minimum difference values are labeled with white boxes. The dihedral angles of red dots are determined by XRD.

Through a similar procedure by scanning frequencies from  $1200 \text{ cm}^{-1}$  to  $3400 \text{ cm}^{-1}$  (fig.2A), the cross angles among other modes were also obtained. For each sample, we collected vibrational cross angles of 12~15 pairs of coupled modes. These experimentally obtained vibrational cross angles are different from the chemical bond cross angles needed for constructing 3D molecular conformations. Theoretical calculations are then used to convert the vibrational angles into bond angles. In doing so, we preset a series of molecular conformations and calculated their vibrational cross angles and compared the calculated angles to the

experimentally measured angles until a minimum was found. The conformations with calculated vibrational angles closest to the measured values were then considered as the most probable conformations experimentally determined. The difference between the calculated and measured vibrational cross angles versus the two dihedral angles is plotted in fig.2(F)~(H) for the three pairs of chiral images in the two crystals (The two pairs of chiral images in the yellow crystal can be individually determined because they have distinct vibrational frequencies for some vibrational modes). The dihedral angles (marked with white boxes in fig.2(F)~(H)) determined in this way are very similar to those determined by XRD (marked with red dots). For the same molecule, we also measured its conformations in liquids with a similar approach. The determined liquid conformations are very similar to those from theoretical calculations. Using the method, the conformation of a ligand molecule on the surface of 4nm Au particle was also determined (fig.3).<sup>5</sup>

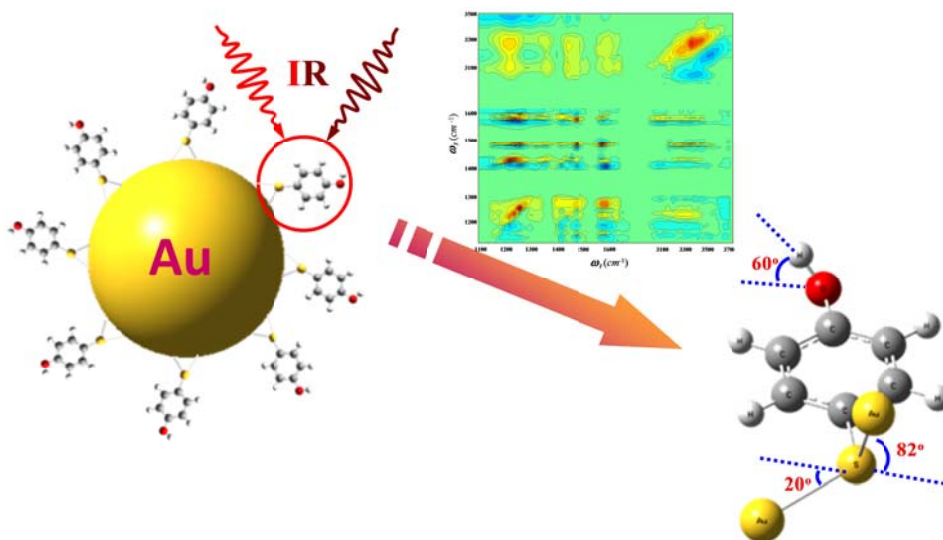


**Figure 3.** Illustration of molecular structure on the surface of 4nm Au particle is determined with the vibrational cross angle method.

## 2.2 Vibrational energy transfer method to determine angstrom molecular distances

The nature of the Born-Oppenheimer Approximation (BOA) is that electrons are much lighter than nuclei so that electronic motions are assumed to be much faster than nuclear motions. In our experiments, the criterion to judge the validity of BOA is whether electronic and nuclear motions are coupled. If they are strongly coupled, the vibrational motions prepared by laser excitation can be converted into electronic motions very fast, resulting in experimentally observed fast vibrational relaxations. However, vibrational relaxations in condensed phases can also be induced by vibration/vibration couplings. To unambiguously distinguish these two origins, we need to understand how vibrational energy transfers because of vibration/vibration couplings. Historically, vibrational energy transfers or relaxations induced by vibration/vibration couplings were described with the correlation formalism or the phonon compensation mechanism or the dark mode formalism. However, none of the previous theoretical approaches is experimentally useful, as they contain too many parameters that cannot be experimentally determined. Therefore, the first step of our experiments is to design experiments to search for the quantitative description of vibrational energy transfers in condensed phases with all parameters that can be experimentally determined. From a series of systematic studies, we have developed a

general theory of which the Forster theory is only an extreme case to quantitatively describe intermolecular vibrational energy transfers<sup>6,7</sup>. The research led to the birth of the vibrational energy transfer angstrom molecular rule method<sup>6,7</sup>. The method was benchmarked with a crystalline sample with known well-defined donor/acceptor distances, as shown in fig.4<sup>6,7</sup>, and successfully applied to investigate ion clustering in strong electrolyte aqueous solutions.<sup>15,16</sup> The results demonstrated that cations directly bind to anions,<sup>9</sup> that mixed ions can segregate because of different water affinities,<sup>10,15</sup> and that organic molecules, that are models of protein building blocks, can directly bind to strong denaturant anions.<sup>11</sup> In contrast to electronic “FRET” which uses large chromophores that can distort structure, the vibrational energy transfer method can use labels that have no effect upon structure. Its chromophores are the chemical bonds themselves. From our research<sup>6,7</sup>, we also found that the previous phonon compensation mechanism to describe intermolecular vibrational energy transfers in liquids was wrong. The dominant vibrational energy transfer mechanism in liquid should be our dephasing mechanism. This is because the spectral diffusion is much faster than the energy transfers so that the modulations by phonons (or instantaneous normal modes) on both energy donor and acceptor cancel out. In other words, phonons have no impact on the energy transfer process. The energy transfer driving force is the frequency fluctuation because of the dephasing events caused by molecular collisions. In solids, phonon modes are long-lived, the dephasing mechanism and the phonon compensation mechanism are competing with each other. Even for the transfers in solids, we found that the majority of previous researchers made a mistake in taking the first order coupling matrix to describe the phonon compensation mechanism for the one phonon process. Instead, the term playing a significant role should be the second order coupling matrix. With our theory, the experimentally observed surprising opposite temperature dependences of resonant and nonresonant energy transfers and inverted energy-gap dependences can be fully explained<sup>6,7</sup>.

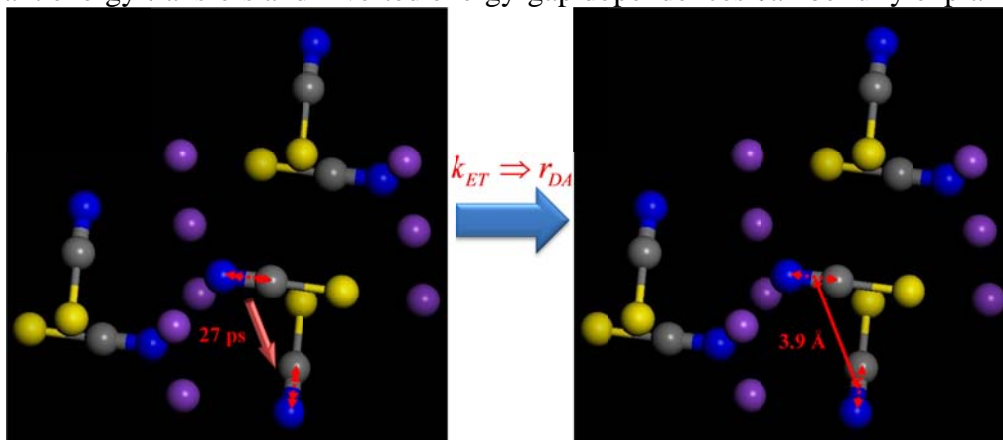


**Figure 4.** Illustration of determining the shortest distance between two anions in KSCN crystal with the vibrational energy transfer method.

### 2.3 Electron/vibrational coupling on surfaces of metal nanomaterials

Equipped with the new spectroscopic setup and the knowledge about vibrational energy transfers, we were ready to investigate the BOA (or electron/vibrational coupling) problem on metal nanomaterial surfaces<sup>12-14</sup>. First of all, we found that the electron/vibrational couplings are particle size dependent (fig.5): when the particle is equal to or larger than 2nm, a strong electron/vibrational coupling is observed. When the particle is smaller than 2nm, no clear

electron/vibrational coupling is observed. The size dependence is the same for Pt, Pd, and Au particles. However, the electron/coupling strengths are very similar in Pt and Pd both of which are much larger than that of Au (fig.6). The observation can be fully explained by the facts: (1) particles larger than 2nm are already metallic so that their surface electronic levels are continuous which can be on resonant with the surface molecular vibration (CO stretch in our studies). Particles smaller than 2nm are semiconductive and their electronic energy levels are much higher than that of the surface molecular vibrations so that resonant energy transfers between surface electrons and vibrations cannot occur. (2) Pt and Pd have similar interaction strengths with surface molecules (CO) by donating d electrons into the antiorbitals of the CO molecules, which is much stronger than that between Au and CO molecules in which the d electron donation doesn't exist. The electron/vibrational coupling is also surface site dependent. On 2nm pt particle surface (fig.7), the order of coupling strengths is hollow>bridge>step> terrace. A similar site dependence is also observed on Pd surfaces. Surface distance dependent measurements show that the energy relaxation rate is approximately proportional to the 2.5<sup>th</sup> power of the distance between the vibrational mode and particle surface, indicating that the electron/vibrational coupling induced relaxation is mainly through the through-bond mechanism (the “mechanical” mechanism rather than the “dipole/dipole” mechanism). Temperature dependent measurements from 80-300K show that the relaxation induced by electron/vibrational coupling is temperature independent, strongly suggesting that this is a resonant transfer process. Because of the size dependent electron/vibrational coupling strengths, the heat generation pathways on the particles are also size dependent. On Pt particles larger than 2nm, heat is generated within a few ps, while it is longer than 50ps on the 1nm particle (fig.8). Based on the results, the energy dissipation pathways are summarized in fig.9.

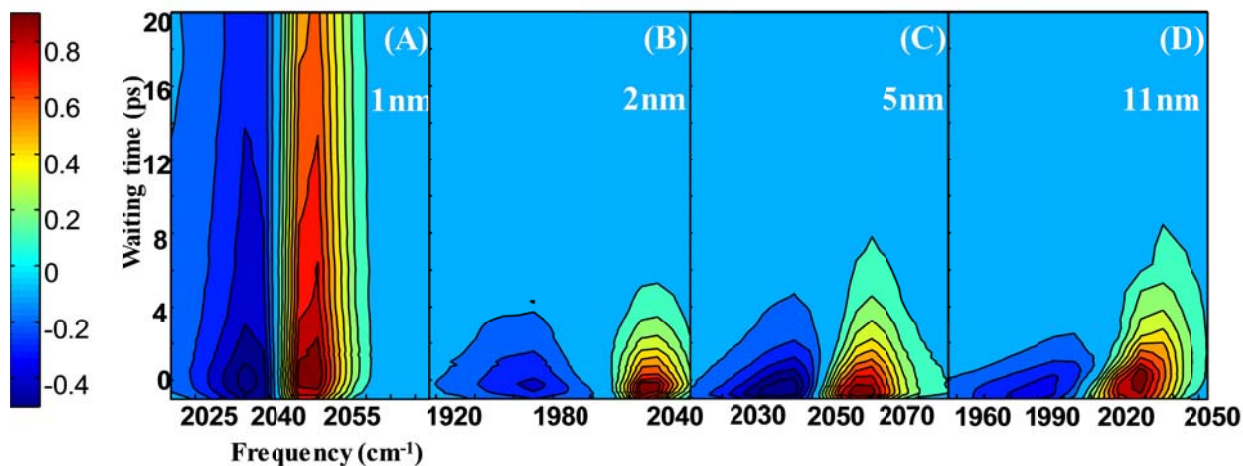


**Figure 5.** The relaxations of CO 1<sup>st</sup> excited state excitation (red: 0-1 transition; blue: 1-2 transition) on the surfaces of Pt particles (step surface site) with different sizes: (A) 1nm, (B) 2nm, (C) 5nm, and (D) 11nm. The results show that the relaxation is much longer on 1nm particle (~35ps). The relaxations on larger particles are much shorter (~2.2ps). The fast decays indicate a very different energy relaxation mechanism on the larger particles – electron/vibrational coupling.

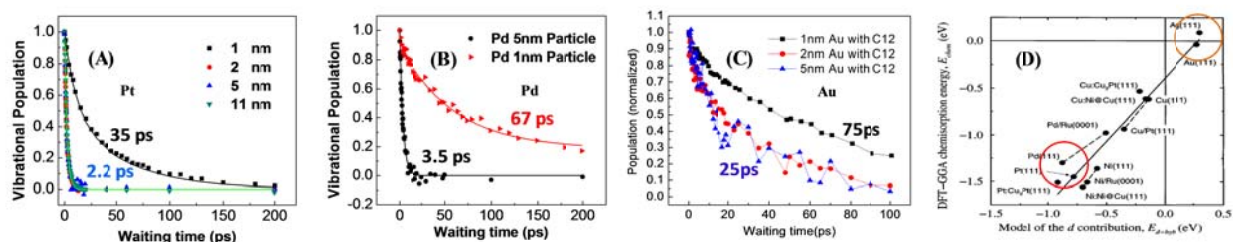


**Figure 6.** CO vibrational relaxation time dynamics on (A) Pt, (B) Pd, and (C) Au nanoparticle surfaces (step surface site). (D) CO/metal interaction strength from literature (PRL. 1996, 2141).

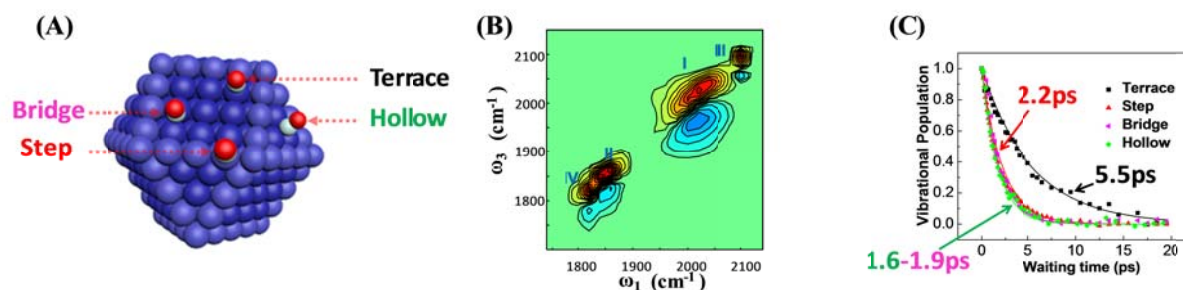


**Figure 7.** (A) Illustration of CO surface sites. (B) 2D IR spectrum of the CO molecules on various sites at 0fs. (C) The vibrational relaxations of CO on various sites.

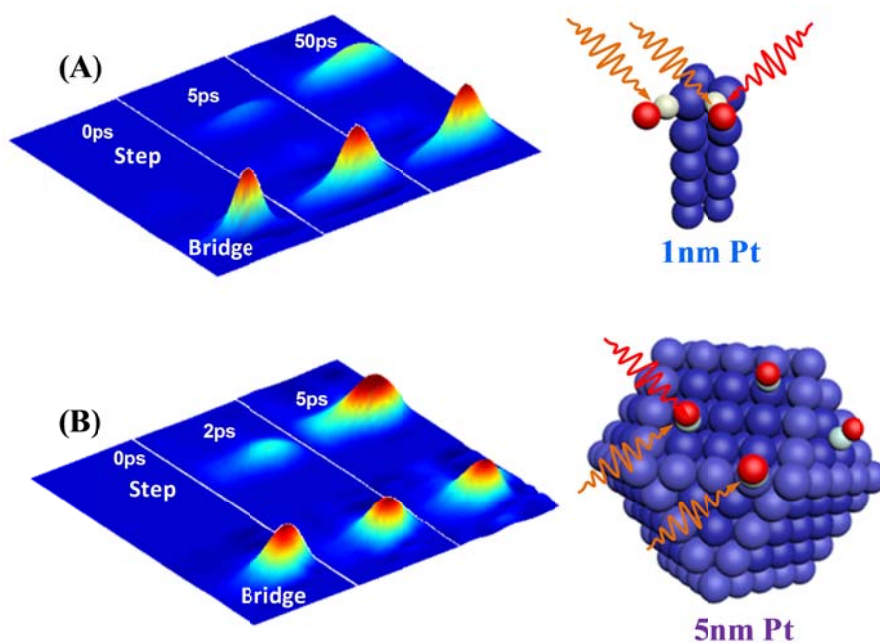


**Figure 8.** Waiting time dependent 2D IR spectra of CO molecules on (A) 1nm Pt, and (B) 5nm Pt surfaces by laser-exciting CO molecules on the bridge sites and detecting the responses on both step and bridge sites. The cross peaks on the step site grow much slower on 1nm particle than 5nm particle, indicating a much slower heat generation.

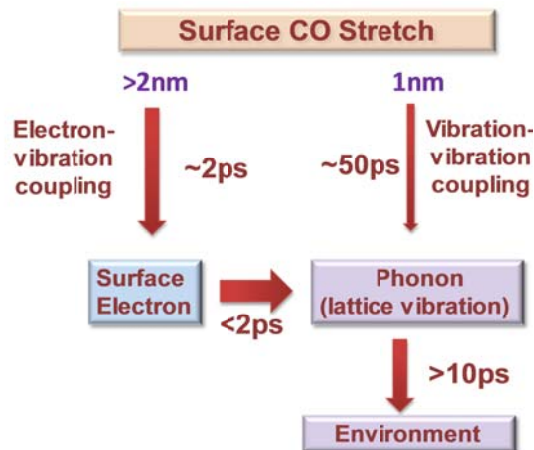


**Figure 9.** Energy dissipation pathways on Pt nanoparticle surfaces.

### 2.3 Publications supported by the award

The following is the list of publications published or to be published supported by the award<sup>1-19</sup>. Some of them were also partially supported by private foundations (Welch and Packard).

- (1) Chen, H. L.; Zhang, Y. F.; Li, J. B.; Liu, H. J.; Jiang, D. E.; Zheng, J. R.: Vibrational Cross Angles in Condensed Molecules: A Structural Tool. *J. Phys. Chem. A* **2013**, *117*, 8407-8415.
- (2) Chen, H. L.; Bian, H. T.; Li, J. B.; Wen, X. W.; Zheng, J. R.: Relative intermolecular orientation probed via molecular heat transport. *J. Phys. Chem. A* **2013**, *117*, 6052-6065.
- (3) Chen, H. L.; Bian, H. T.; Li, J. B.; Wen, X. W.; Zheng, J. R.: Ultrafast multiple-mode multiple-dimensional vibrational spectroscopy. *Inter. Rev. Phys. Chem.* **2012**, *31*, 469-565.
- (4) Chen, H. L.; Bian, H. T.; Li, J. B.; Guo, X. M.; Wen, X. W.; Zheng, J. R.: Molecular Conformations of Crystalline L-Cysteine Determined with Vibrational Cross Angle Measurements. *J. Phys. Chem. B* **2013**, *117*, 15614-15624.
- (5) Bian, H. T.; Li, J. B.; Chen, H. L.; Yuan, K. J.; Wen, X. W.; Li, Y. Q.; Sun, Z. G.; Zheng, J. R.: Molecular Conformations and Dynamics on Surfaces of Gold Nanoparticles Probed with Multiple-Mode Multiple-Dimensional Infrared Spectroscopy. *Journal of Physical Chemistry C* **2012**, *116*, 7913-7924.
- (6) Chen, H. L.; Wen, X. W.; Guo, X. M.; Zheng, J. R.: Intermolecular Vibrational Energy Transfers in Liquids and Solids. *Phys. Chem. Chem. Phys.* **2014**, *16*, 13995-14014.
- (7) Chen, H. L.; Wen, X. W.; Li, J. B.; Zheng, J. R.: Molecular distances determined with resonant vibrational energy transfers. *J. Phys. Chem. A* **2014**, *118*, 2463-2469.
- (8) Bian, H. T.; Chen, H. L.; Li, J. B.; Wen, X. W.; Zheng, J. R.: Nonresonant and resonant mode-specific intermolecular vibrational energy transfers in electrolyte aqueous solutions. *J. Phys. Chem. A* **2011**, *115*, 11657-11664.

- (9) Li, J. B.; Bian, H. T.; Chen, H. L.; Hoang, B.; Zheng, J. R.: Ion Association in Aqueous Solutions Probed through Vibrational Energy Transfers among Cation, Anion and Water Molecules. *J. Phys. Chem. B.* **2013**, *117*, 4274 - 4283.
- (10) Bian, H. T.; Li, J. B.; Zhang, Q.; Chen, H. L.; Zhuang, W.; Gao, Y. Q.; Zheng, J. R.: Ion Segregation in Aqueous Solutions. *J. Phys. Chem. B* **2012**, *116*, 14426-14432.
- (11) Li, J. B.; Bian, H. T.; Wen, X. W.; Chen, H. L.; Yuan, K. J.; Zheng, J. R.: Probing Ion/Molecule Interactions in Aqueous Solutions with Vibrational Energy Transfer. *J. Phys. Chem. B.* **2012**, *116*, 12284-12294.
- (12) Li, J. B.; Qian, H. F.; Chen, H. L.; Zhao, Z.; Yuan, K. J.; Chen, G. X.; Miranda, A.; Guo, X. M.; Jiang, D. E.; ZHeng, N. F.; Wong, M. S.; Zheng, J. R.: Two Distinctive Energy Dissipation Pathways of Monolayer Molecules on Metal Nanoparticle Surfaces. *To be submitted* **2014**.
- (13) Li, J. B.; Wang, J. K.; Chen, H. L.; Zhao, Z.; Qian, H. F.; Wen, X. W.; Bian, H. T.; Wong, M. S.; Zheng, J. R.: Temperature and Site Dependence of Surface Electron/Vibration Coupling on Platinum Nanoparticles Coated with Carbon Monoxide. *To be submitted* **2014**.
- (14) Li, J. B.; Qian, H. F.; Wong, M. S.; Zheng, J. R.: Fast Vibrational Relaxations on Pt, Au, and Pd Nanoparticle Surfaces. *Under preparation* **2014**.
- (15) Bian, H. T.; Chen, H. L.; Zhang, Q.; Li, J. B.; Wen, X. W.; Zhuang, W.; Zheng, J. R.: Cation Effects on Rotational Dynamics of Anions and Water Molecules in Alkali (Li<sup>+</sup>, Na<sup>+</sup>, K<sup>+</sup>, Cs<sup>+</sup>) Thiocyanate (SCN<sup>-</sup>) Aqueous Solutions *J. Phys. Chem. B.* **2013**, *117*, 7972 - 7984.
- (16) Zhang, Q.; Xie, W. J.; Bian, H. T.; Gao, Y. Q.; Zheng, J. R.; Zhuang, W.: Microscopic Origin of the Deviation from Stokes-Einstein Behavior Observed in Dynamics of the KSCN Aqueous Solutions: A MD simulation study. *J. Phys. Chem. B.* **2013**, *117*, 2992-3004.
- (17) Yuan, K. J.; Bian, H. T.; Shen, Y. N.; Jiang, B.; Li, J. B.; Zhang, Y. F.; Chen, H. L.; Zheng, J. R.: Coordination Number of Li<sup>+</sup> in Nonaqueous Electrolyte Solutions Determined by Molecular Rotational Measurements. *J. Phys. Chem. B.* **2014**, *118*, 3689-3695.
- (18) Nickel, D. V.; Delaney, S. P.; Bian, H. T.; Zheng, J. R.; Korter, T. M.; Mittleman, D. M.: Terahertz Vibrational Modes of the Rigid Crystal Phase of Succinonitrile. *J. Phys. Chem. A.* **2014**, *118*, 2442-2446.
- (19) Li, J. B.; Qian, H. F.; Wong, M. S.; Zheng, J. R.: Vibrational excitation induced molecular hopping on nanoparticle surfaces. *Under preparation* **2014**.